Structural and Photophysical Properties of Mononuclear and Dinuclear Lanthanide(III) Complexes of Multidentate Podand Ligands Based on Poly(pyrazolyl)borates

Nicola Armaroli,*,† Gianluca Accorsi,† Francesco Barigelletti,† Samantha M. Couchman,‡ James S. Fleming,‡ Nicholas C. Harden,‡ John C. Jeffery,‡ Karen L. V. Mann,‡ Jon A. McCleverty,*,‡ Leigh H. Rees,‡ Sarah R. Starling,‡ and Michael D. Ward*,‡

Istituto di Fotochimica e Radiazioni d'Alta Energia del CNR, Via Gobetti 101, 40129 Bologna, Italy, and School of Chemistry, University of Bristol, Cantock's Close, Bristol BS8 1TS, U.K.

Received June 17, 1999

Lanthanide(III) complexes have been prepared with $[L^1]^-$ [the tetradentate chelating ligand bis{3-(2-pyridyl)-pyrazolyl}dihydroborate], $[L^2]^-$ [the tetradentate chelating ligand bis{3-(2-pyrazinyl)pyrazolyl}dihydroborate], $[L^3]^-$ [the hexadentate chelating ligand bis[3-{6′-(2,2′-bipyridyl)}pyrazol-1-yl]dihydroborate], and $[L^4]^{2-}$ [the 12-dentate compartmental ligand hexakis{3-(2-pyridyl)pyrazol-1-yl}diboran(IV)ate, which has two hexadentate tris-(pyrazolyl)borate-based cavities linked "back-to-back" by a B−B bond]. $[Ln(L^1)_2(NO_3)]$ are 10-coordinate with two tetradentate N-donor ligands and one bidentate nitrate. $[Ln(L^2)_2(NO_3)]$ have 10-coordinate structures similar to those of the $[L^1]^-$ complexes except that the coordinated N^1 of the pyrazine rings is not such a good donor as the pyridine rings in the $[L^1]^-$ complexes, leading to marked lengthening of these Ln−N bonds. $[Ln(L^3)(NO_3)_2]$ are also 10-coordinate from one hexadentate chelating ligand which has a pseudoequatorial coordination mode and two pseudoaxial bidentate nitrate ligands; the hexadentate ligand has a shallow helical twist to prevent steric interference between its ends. Finally $[\{Ln(NO_3)_2(L^4)]$ are dinuclear, with each metal center being 10-coordinate from a tripodal hexadentate ligand cavity and two bidentate nitrates. Five complexes were structurally characterized: $[Tb(L^2)_2(NO_3)]\cdot$dmf is monoclinic ($P2_1/c$) with $a = 14.881(3)$ Å, $b = 15.5199(12)$ Å, $c = 15.845(2)$ Å, $\beta = 92.387(12)°$, and $Z = 4$. $[Gd(L^2)_2(NO_3)]\cdot$dmf is monoclinic ($P2_1/c$) with $a = 14.926(2)$ Å, $b = 15.465(2)$ Å, $c = 15.878(2)$ Å, $\beta = 92.698(11)°$, and $Z = 4$. $[Eu(L^3)(NO_3)_2]\cdot$dmf·0.5Et_2O is triclinic ($P\bar{1}$) with $a = 10.020(3)$ Å, $b = 13.036(3)$ Å, $c = 14.740(3)$ Å, $\alpha = 70.114(14)°$, $\beta = 71.55(2)°$, $\gamma = 79.66(2)°$, and $Z = 2$. $[\{La(NO_3)-(dmf)_2\}_2(L^4)](NO_3)_2\cdot$dmf is orthorhombic ($Pbca$) with $a = 18.813(2)$ Å, $b = 15.241(2)$ Å, $c = 27.322(2)$, and $Z = 4$. $[\{Gd(NO_3)_2\}_2(L^4)]\cdot$2.4dmf is tetragonal ($P4_2/n$) with $a = 16.622(6)$, $c = 24.19(5)$ Å, and $Z = 4$. Detailed photophysical studies have been performed on the free ligands and their complexes with Gd(III), Eu(III), and Tb(III) in several solvents. The results show a wide range in the emission properties of the complexes which can be rationalized in terms of subtle variations in the steric and electronic properties of the ligands. In particular the dinuclear Tb(III) complex of $[L^4]^{2-}$ has an emission quantum yield of ca. 0.5 in D_2O and MeOD.

Introduction

Complexes of lanthanide ions continue to attract intense interest because of their important practical applications.[1,2] In particular Eu^{3+} and Tb^{3+} are characterized by long-lived (millisecond time scale) and strongly luminescent electronically excited states, which makes them appealing for analytical purposes, especially in the biomedical field.[1,3,4] Exploitation of this luminescence requires ligands with specific properties. First, the ligand must have a large absorption cross section, to sensitize by ligand-to-metal energy-transfer the luminescent f−f excited states of the metal ions which are not readily accessible by direct excitation. This is most easily achieved by using aromatic ligands which absorb light strongly in the UV region. Second, the ligand must have a high denticity in order to encapsulate the metal ion and protect it from solvent interactions, which can deactivate its excited state via nonradiative processes.[3] Very many lanthanide complexes have been prepared using ligands which obey these broad criteria.[5] We have been interested in the synthesis and characterization of lanthanide complexes of multidentate podand ligands based on the tris(pyrazolyl)borate core[6−10] and, in particular, have recently described the detailed photophysical properties of lanthanide complexes of the tris-

* Corresponding authors. E-mail: armaroli@frae.bo.cnr.it; mike.ward@bristol.ac.uk.

† Istituto FRAE, Bologna.

‡ University of Bristol.

(1) Parker, D.; Williams, J. A. G. *J. Chem. Soc., Dalton Trans.* **1996**, 3613.

(2) Aime, S.; Botta, M.; Fasano, M.; Terreno, E. *Chem. Soc. Rev.* **1998**, *27*, 19.

(3) Sabbatini, N.; Guardigli, M.; Lehn, J.-M. *Coord. Chem. Rev.* **1993**, *123*, 201.

(4) Sabbatini, N.; Guardigli, M.; Manet, I. In *Handbook on The Physics and Chemistry of Rare Earths*; Gschneidner, K. A., Jr., Eyring, L., Eds.; Elsevier: Amsterdam, 1996; Vol. 23.

(5) See, for example: (a) Prodi, L.; Maestri, M.; Ziessel, R.; Balzani, V. *Inorg. Chem.* **1991**, *30*, 3798. (b) Wu, S. L.; Horrocks, DeW., Jr. *J. Chem. Soc., Dalton Trans.* **1997**, 1497. (c) van der Tol, E. B.; van Ramesdonk, H. J.; Verhoeven, J. W.; Steemers, F. J.; Kerver, E. G.; Verboom, W.; Reinhoudt, D. N. *Chem. Eur. J.* **1998**, *4*, 2315. (d) de Silva, A. P.; Gunaratne, H. Q. N.; Rice, T. E.; Steward, S. *Chem. Commun.* **1997**, 1891. (e) Wolbers, M. P. O.; van Veggel, F. C. J. M.; Snellink-Ruël, B. H. M.; Hofstraat, J. W.; Guerts, F. A. J.; Reinhoudt, D. N. *J. Am. Chem. Soc.* **1997**, *119*, 138. (f) Ulrich, G.; Ziessel, R.; Manet, I.; Guardigli, M.; Sabbatini, N.; Fraternali, F.; Wipff, G. *Chem. Eur. J.* **1997**, *3*, 1815. (g) Martin, N.; Bünzli, J.-C. G.; McKee, V.; Piguet, C.; Hopfgartner, G. *Inorg. Chem.* **1998**, *37*, 577. (h) Lata, M.; Takalo, H.; Mukkala, V.-M.; Kankare, J. *Inorg. Chim. Acta* **1998**, *267*, 63.

10.1021/ic990708i CCC: $18.00
Published on Web 11/12/1999

Chart 1

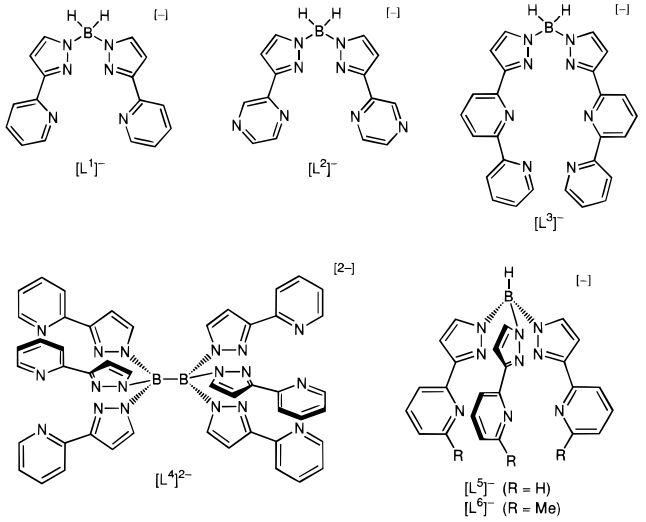

(pyrazolyl)borates $[L^5]^-$ and $[L^6]^-$ (Chart 1).[7,10] The combination of the all-nitrogen donor set and the negative charge makes these effective ligands for the hard 3+ lanthanide ions, and some of the complexes we have examined show intense metal-centered luminescence, assisted by near-complete encapsulation of the metal centers such that relatively few sites are available for solvent-based deactivation. We describe in this paper the syntheses, structures, and photophysical properties of four series of lanthanide complexes of the ligands $[L^1]^-$−$[L^4]^{2-}$ (Chart 1) which are all based on bis- or tris(pyrazolyl)borate cores. Additional heterocyclic donors (pyridyl or pyrazinyl) are attached to the C^3 positions of the pyrazolyl rings, such that each ligand contains two or more bidentate or terdentate chelating "arms" linked by a boron headgroup. Ligands $[L^1]^-$−$[L^3]^-$ form mononuclear lanthanide(III) complexes by chelation to a single metal ion, whereas $[L^4]^{2-}$ is a binucleating ligand that has two distinct hexadentate compartments. A few of these complexes have been prepared before, but no detailed photophysical studies have been carried out until now; the remaining complexes are reported here for the first time, and the crystal structures of five of the new complexes are reported.

Results and Discussion

Syntheses and Structures of Lanthanide Complexes of $[L^1]^-$, $[L^2]^-$, and $[L^3]^-$. The lanthanide complexes of $[L^1]^-$ that we investigated are of the form $[M(L^1)_2(NO_3)_2]$ and are 10-coordinate in the solid state with two tetradentate chelating ligands L^1 and a bidentate nitrate ligand. The synthesis and crystal structure of $[Tb(L^1)_2(NO_3)_2]\cdot 2CH_2Cl_2$ has been reported,[8] but the Eu^{3+} and Gd^{3+} analogues are new and were simply prepared by reaction of KL^1 with the appropriate lanthanide nitrate hydrate. The formulation of these complexes was confirmed by elemental analyses and FAB mass spectrometry (Table 1).

Ligand $[L^2]^-$ is similar to $[L^1]^-$ in that it has a tetradentate bonding pocket, but it contains pyrazinyl donors in place of pyridyl donors such that there are externally directed N atoms at position 4 of the pyrazinyl ring.[11] This could alter the coordination mode of the ligand compared to $[L^1]^-$ if the externally directed N atom acts as a bridge to another metal ion, as we recently observed with a Pb(II) complex of $[L^2]^-$.[11] However reaction of KL^2 with lanthanide nitrate hydrate salts afforded $[M(L^2)_2(NO_3)]$ (M = Eu, Gd, Tb) in which $[L^2]^-$, like $[L^1]^-$,[8] acts only as a tetradentate chelate and the externally directed N atoms of the pyrazinyl rings are not involved in bridging interactions. Again FAB mass spectra and elemental analyses provided the principal characterization; two of the complexes were also structurally characterized.

The crystal structure of $[Tb(L^2)_2(NO_3)]\cdot$dmf is shown in Figure 1 (see also Tables 2 and 3); the crystal structure of $[Gd(L^2)_2(NO_3)]\cdot$dmf was also determined and is essentially identical, being isostructural and isomorphous, and is therefore not shown. The structures are generally similar to those of the lanthanide complexes with $[L^1]^-$, with one important exception described below.[8] Each ligand coordinates both bidentate arms to the lanthanide ion, such that the metal ions are 10-coordinate from two tetradentate ligands $[L^2]^-$ and one bidentate nitrate ion. Each bidentate pyrazolyl−pyrazine arm is approximately planar (twists between adjacent pyrazinyl and pyrazolyl rings ≤ 6°), but the two arms of each ligand are inclined at 50−60° to one another because of the tetrahedral boron atom which gives each ligand a "folded" conformation. The main difference between the structures of these complexes with $[L^2]^-$ and the related complexes with $[L^1]^-$ is that the metal−N(pyrazine) distances of $[Tb(L^2)_2(NO_3)]\cdot$dmf are significantly longer than the metal−N(pyridine) distances of $[Tb(L^1)_2(NO_3)]\cdot(CH_2Cl_2)_2$, by ca. 0.1 Å on average. In contrast the metal−N(pyrazolyl) distances are comparable between the two sets of complexes. This indicates that the pyrazinyl group of L^2 is a poorer σ-donor than the pyridyl group of L^1, which is in agreement with the known pK_a values of pyridine (5.2) and pyrazine (0.6) and has important consequences for the luminescence characteristics of these complexes (see later).

Ligand $[L^3]^-$ is hexadentate, having two terdentate arms; while it can bridge two metal ions to give dinuclear double helicates with K^+ and Cu^{2+}, it coordinates to a single lanthanide ion to give complexes of the type $[M(L^3)(NO_3)_2]$ in which the bidentate nitrates are in pseudoaxial positions with the hexadentate $[L^3]^-$ wrapped around the "equator".[12] The synthesis and crystal structure of $[Gd(L^3)(NO_3)_2]$ was described previously,[12] but the analogues with Eu^{3+} and Tb^{3+} are new and were simply prepared by reaction of $K_2(L^3)_2$ with the appropriate lanthanide nitrate hydrate. FAB mass spectra of these complexes showed strong peaks for both the molecular ion and for a fragment arising from loss of one nitrate ion (Table 1). The crystal structure of $[Eu(L^3)(NO_3)_2]\cdot$dmf$\cdot 0.5Et_2O$ is shown in Figure 2 (see also Table 4) and is generally similar to the structure of the Gd(III) analogue described earlier. The metal center is 10-coordinate, from one hexadentate N-donor ligand $[L^3]^-$ and two bidentate nitrates. The hexadentate ligand approximately forms a pseudoequatorial belt, with the two nitrate ions in the "axial" positions. To prevent unfavorable steric interactions between the two termini of $[L^3]^-$ which are directed toward each other, the ligand adopts a shallow monohelical twist

(6) Jones, P. L.; Amoroso, A. J.; Jeffery, J. C.; McCleverty, J. A.; Psillakis, E.; Rees, L. H.; Ward, M. D. *Inorg. Chem.* **1997**, *36*, 10.
(7) Armaroli, N.; Balzani, V.; Barigelletti, F.; Ward, M. D.; McCleverty, J. A. *Chem. Phys. Lett.* **1997**, *276*, 435.
(8) Bardwell, D. A.; Jeffery, J. C.; Jones, P. L.; McCleverty, J. A.; Psillakis, E.; Reeves, Z.; Ward, M. D. *J. Chem. Soc., Dalton Trans.* **1997**, 2079.
(9) Harden, N. C.; Jeffery, J. C.; McCleverty, J. A.; Rees, L. H.; Ward, M. D. *New J. Chem.* **1998**, *22*, 661.
(10) Reeves, Z. R.; Mann, K. L. V.; Jeffery, J. C.; McCleverty, J. A.; Ward, M. D.; Barigelletti, F.; Armaroli, N. *J. Chem. Soc., Dalton Trans.* **1999**, 349.
(11) Mann, K. L. V.; Jeffery, J. C.; McCleverty, J. A.; Ward, M. D. *Polyhedron* **1999**, *18*, 721.
(12) Fleming, J. S.; Psillakis, E.; Couchman, S. M.; Jeffery, J. C.; McCleverty, J. A.; Ward, M. D. *J. Chem. Soc., Dalton Trans.* **1998**, 537.

Table 1. Analytical and Mass Spectroscopic Data for the New Complexes

complex	analysis[a] (%)			*m/z* (rel intensity)	
	C	H	N	M^+	$[M - NO_3]^+$
$[Eu(L^1)_2(NO_3)]$	46.4 (47.1)	3.5 (3.4)	21.9 (22.3)	758 (80%)[b]	
$[Gd(L^1)_2(NO_3)]$	46.3 (46.8)	3.2 (3.4)	22.5 (22.2)	762 (60%)[b]	
$[Eu(L^2)_2(NO_3)]$	41.5 (41.0)	3.3 (2.9)	28.7 (29.0)	759 (90%)[b]	
$[Gd(L^2)_2(NO_3)]$	40.9 (40.7)	3.3 (2.9)	28.0 (28.8)	763 (35%)[b]	
$[Tb(L^2)_2(NO_3)]$	40.0 (40.6)	2.6 (2.9)	28.2 (28.8)	765 (100%)[b]	
$[Eu(L^3)(NO_3)_2]$	41.8 (42.7)	2.7 (2.7)	18.7 (19.2)	731 (5%)	670 (25%)[c]
$[Tb(L^3)(NO_3)_2]$	41.5 (42.3)	2.7 (2.7)	18.8 (19.0)	738 (10%)	676 (80%)[c]
$[\{La(NO_3)_2\}_2(L^4)]$	*d*				1351 (20%)[c]
$[\{Eu(NO_3)_2\}_2(L^4)]$	39.9 (40.1)	3.0 (2.5)	21.4 (21.4)	1436 (5%)[c]	
$[\{Gd(NO_3)_2\}_2(L^4)]$	39.1 (39.8)	2.0 (2.5)	21.8 (21.3)		1386 (20%)[c]
$[\{Tb(NO_3)_2\}_2(L^4)]$	39.3 (39.7)	2.6 (2.5)	21.1 (21.2)	1452 (5%)[c]	

[a] Calculated values in parentheses. [b] FAB mass spectrum. [c] Electrospray mass spectrum. [d] Reliable elemental analysis could not be obtained for this complex (see ref 6).

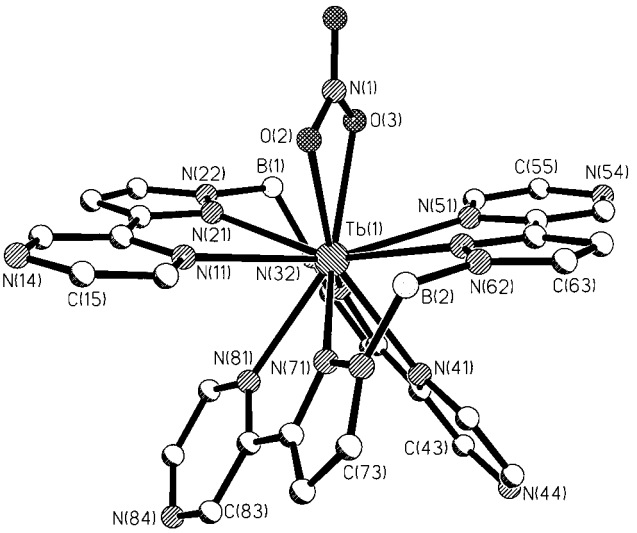

Figure 1. Crystal structure of $[Tb(L^2)_2(NO_3)]\cdot$dmf. (The Gd^{3+} analogue is isostructural and isomorphous.)

such that the terminal pyridyl rings are offset above and below the average equatorial plane. The bond distances and angles are similar to those of $[Gd(L^3)(NO_3)_2]$.[12]

Synthesis of $[L^4]^{2-}$ and the Structures of Its Dinuclear Lanthanide Complexes. Despite the enduring popularity of tris(pyrazolyl)borate ligands (generically Tp), virtually all published work with them relates to mononuclear complexes;[13] incorporation of Tp units into multinucleating bridging ligands is very rare because of the synthetic difficulties involved. There are just two examples of dinucleating bridging ligands based on Tp fragments: $[\{C_5H_4[B(pz)_3]\}_2Fe]^{2-}$, in which the two Tp fragments are attached to the cyclopentadienyl rings of a central ferrocenyl moiety which therefore acts as a "ball-bearing" spacer,[14] and $[(pz)_3B-B(pz)_3]^{2-}$, in which the two Tp fragments are linked back-to-back directly by a B−B bond.[15] This is in strong contrast to e.g. oligopyridyl ligands, where it is synthetically straightforward to link together two chelating fragments to give "back-to-back" ligands (usually, bis(terpyridines)) for the preparation of multinuclear complexes, and the use of such bridging ligands to study electronic and magnetic metal−metal interactions is now commonplace.[16] In a recent preliminary communication[8] we described the preparation of the ligand $[L^4]^{2-}$, which contains two hexadentate pockets based on pyridyl-substituted Tp groups linked by a B−B bond and is designed to allow synthesis of dinuclear lanthanide(III) complexes for this study. Dinuclear lanthanide complexes are rare; the most obvious examples are the dinuclear triple helicates of Piguet et al.[17]

Reaction of K_2L^4 with various lanthanide(III) nitrates in methanol afforded white precipitates of materials whose mass spectra and elemental analyses (Table 1) indicated the formulation $[\{M(NO_3)_2\}L^4]$, with one $\{M(NO_3)_2\}^+$ fragment coordinated in each hexadentate pocket (by analogy with the complexes of the hexadentate podand ligand tris[3-(2-pyridyl)-pyrazolyl]hydroborate, L^5).[6] For this series of complexes we found that electrospray mass spectrometry gave better results than FAB mass spectrometry. Even so, the molecular ions are in each case very weak and there is much more evidence for substantial fragmentation than occurred with the mononuclear complexes described earlier.

Final confirmation of the nature of these complexes was provided by two crystal structures of the La and Gd complexes; see Figures 3 and 4 and Tables 2 and 5. The structure of $[\{Gd(NO_3)_2\}L^4]\cdot 2.4$dmf (Figure 3) is a poor one ($R_1 = 10.7\%$) because of the instability of the crystal and the presence of extensive disorder which rendered diffraction very weak (see Experimental Section). For this reason it is not appropriate to discuss the metrical parameters in any detail, but the gross structure is clear. Each Gd(III) ion is located in one hexadentate cavity of the ligand, with two bidentate nitrates completing the 10-coordinate geometry, and the coordination environment around each metal is basically the same as was observed in the analogous mononuclear lanthanide complexes $[M(L^5)(NO_3)_2]$.[6] For obvious steric reasons the two sets of three pyrazolyl groups are mutually staggered about the B−B bond. The two metal centers are crystallographically equivalent, with a C_2 axis bisecting the B−B bond. The metal−metal separation is 9.45 Å.

Recrystallization of $[\{La(NO_3)_2\}L^4]$ from dmf/ether in the same way afforded much better crystals of $[\{La(NO_3)(dmf)_2\}_2(L^4)](NO_3)_2\cdot$dmf (Figure 4). The main difference between this structure and the previous one is that at each metal site one of the nitrate ligands has been replaced by two molecules of dmf from the recrystallization solvent molecules which act as

(13) Trofimenko, S. *Chem. Rev.* **1993**, *93*, 943.
(14) de Biani, F. F.; Jäckle, F.; Spiegler, M.; Wagner, M.; Zanello, P. *Inorg. Chem.* **1997**, *36*, 2103.
(15) Brock, C. P.; Das, M. K.; Minton, R. P.; Niedenzu, K. *J. Am. Chem. Soc.* **1988**, *110*, 817.
(16) (a) Balzani, V.; Juris, A.; Venturi, M.; Campagna, S.; Serroni, S. *Chem. Rev.* **1996**, *96*, 759. (b) Ward, M. D. *Chem. Soc. Rev.* **1995**, *24*, 121.
(17) (a) Elhabiri, M.; Scopellitti, R.; Bünzli, J.-C. G.; Piguet, C. *Chem. Commun.* **1998**, 2347. (b) Martin, N.; Bünzli, J.-C. G.; McKee, V.; Piguet, C.; Hopfgartner, G. *Inorg. Chem.* **1998**, *37*, 577. (c) Piguet, C.; Bünzli, J.-C. G. Bernardinelli, G.; Hopfgartner, G.; Williams, A. F. *J. Am. Chem. Soc.* **1993**, *115*, 8197.

Table 2. Crystallographic Data for the Five Crystal Structures.

	compound				
	$[Tb(L^2)_2(NO_3)]\cdot dmf$	$[Gd(L^2)_2(NO_3)]\cdot dmf$	$[Eu(L^3)(NO_3)_2]\cdot dmf\cdot 0.5Et_2O$	$[\{La(NO_3)(dmf)_2\}_2(L^4)](NO_3)_2\cdot dmf$	$[\{Gd(NO_3)_2\}_2(L^4)]\cdot 2.4dmf$
empirical formula	$C_{31}H_{31}B_2N_{18}O_4Tb$	$C_{31}H_{31}B_2GdN_{18}O_4$	$C_{31}H_{32}BEuN_{11}O_{7.5}$	$C_{63}H_{71}B_2La_2N_{27}O_{17}$	$C_{55.2}H_{52.8}B_2Gd_2N_{24.4}O_{14.4}$
fw	900.28	898.61	841.45	1777.91	1624.54
cryst dimens (mm)	0.38 × 0.14 × 0.12	0.40 × 0.18 × 0.12	0.20 × 0.11 × 0.10	0.22 × 0.20 × 0.10	0.15 × 0.10 × 0.05
cryst system	monoclinic	monoclinic	triclinic	orthorhombic	tetragonal
space group	$P2_1/c$	$P2_1/c$	$P\bar{1}$	$Pbca$	$P4_2/n$
a (Å)	14.881(3)	14.926(2)	10.020(3)	18.813(2)	16.622(6)
b (Å)	15.5199(12)	15.465(2)	13.036(3)	15.241(2)	16.622(4)
c (Å)	15.845(2)	15.878(2)	14.740(3)	27.322(2)	24.19(5)
α (deg)			70.114(14)		
β (deg)	92.387(12)	92.698(11)	71.55(2)		
γ (deg)			79.66(2)		
V (Å^3)	3654.9(8)	3661.1(8)	1712.0(7)	7836(2)	6682(5)
Z	4	4	2	4	4
ρ_{calcd} (g/cm^3)	1.636	1.630	1.632	1.507	1.615
abs coeff (mm^{-1})	2.000	1.876	1.898	1.157	2.049
F(000)	1800	1796	846	3592	3232
T (K)	173	173	173	173	173
λ (Å)	0.710 73	0.710 73	0.710 73	0.710 73	0.710 73
reflcns collcd: tot./indepd/R_{int}	22980/8358/0.0396	22719/8322/0.0320	17765/7727/0.0911	47192/8988/0.0309	21321/3124/0.2547
2θ limit for data (deg)	55	55	55	55	40
data/restraints/params	8358/30/507	8322/0/505	7727/0/480	8988/0/523	3059/477/600
final R1, wR2[a,b]	0.0372, 0.0823	0.0299, 0.0727	0.0513, 0.1329	0.0323, 0.1004	0.1072, 0.2559
a, b for weighting scheme[b]	0.0368, 0	0.0355, 0	0.0530, 0	0.0510, 10.910	0.0351, 359.744
largest peak, hole (e/Å^3)	+1.298, −1.273	+1.127, −0.981	+1.206, −0.865	+0.992, −0.409	+1.276, −0.771

[a] Structure was refined on F_o^2 using all data; the value of R1 is given for comparison with older refinements based on F_o with a typical threshold of $F = 4\sigma(F)$. [b] $wR_2 = [\sum w(F_o^2 - F_c^2)^2]/\sum w(F_o^2)^2]^{1/2}$, where $w^{-1} = [\sigma^2(F_o^2) + (aP)^2 + bP]$ and $P = [\max(F_o^2, 0) + 2F_c^2]/3$.

Table 3. Selected Bond Distances (Å) and Angles (deg) for $[M(L^2)_2(NO_3)]\cdot dmf$ (M = Gd, Tb)

Metal−Oxygen Distances			
Gd(1)−O(2)	2.532(2)	Tb(1)−O(2)	2.490(3)
Gd(1)−O(3)	2.508(2)	Tb(1)−O(3)	2.508(3)
Metal−N(pyrazolyl) Distances			
Gd(1)−N(21)	2.605(3)	Tb(1)−N(21)	2.568(3)
Gd(1)−N(31)	2.522(2)	Tb(1)−N(31)	2.508(3)
Gd(1)−N(61)	2.584(3)	Tb(1)−N(61)	2.591(3)
Gd(1)−N(71)	2.523(2)	Tb(1)−N(71)	2.501(3)
Metal−N(pyrazinyl) Distances			
Gd(1)−N(11)	2.827(3)	Tb(1)−N(11)	2.815(3)
Gd(1)−N(41)	2.640(2)	Tb(1)−N(41)	2.625(3)
Gd(1)−N(51)	2.804(3)	Tb(1)−N(51)	2.848(3)
Gd(1)−N(81)	2.640(3)	Tb(1)−N(81)	2.629(3)
Bite Angles within Each Chelating Ligand			
O(2)−Gd(1)−O(3)	50.33(8)	O(2)−Tb(1)−O(3)	50.68(9)
N(11)−Gd(1)−N(21)	60.21(8)	N(11)−Tb(1)−N(21)	60.97(10)
N(21)−Gd(1)−N(31)	70.74(8)	N(21)−Tb(1)−N(31)	71.30(10)
N(31)−Gd(1)−N(41)	63.69(8)	N(31)−Tb(1)−N(41)	64.11(10)
N(51)−Gd(1)−N(61)	60.91(8)	N(51)−Tb(1)−N(61)	60.13(10)
N(61)−Gd(1)−N(71)	70.94(8)	N(61)−Tb(1)−N(71)	71.03(10)
N(71)−Gd(1)−N(81)	63.80(8)	N(71)−Tb(1)−N(81)	63.87(10)

monodentate O-donor ligands. Each metal ion is again 10-coordinate with an N_6O_4 coordination environment, arising from the hexadentate N-donor cavity of $[L^4]^{2-}$, one bidentate nitrate ligand, and the two dmf ligands; the remaining nitrate ion (and half a dmf molecule per metal) are free in the crystal lattice. The complex lies astride an inversion center which is at the center of the B−B bond, such that the two ends are crystallographically equivalent. The La···La separation is 9.671 Å. Finally, comparison of the metal−ligand bond lengths between the Gd^{3+} and La^{3+} complexes clearly shows the effects of the lanthanide contraction.

Absorption Spectra of the Complexes. For discussion of the photophysical properties of the complexes we use the following abbreviations: M·L[1] for $[M(L^1)_2(NO_3)]$; M·L[2] for $[M(L^2)_2(NO_3)]$; M·L[3] for $[M(L^3)(NO_3)_2]$; $M_2\cdot L^4$ for $[\{M(NO_3)_2\}L^4]$. In addition, references to the "free ligands" $[L^1]^-$ to $[L^4]^{2-}$ actually refer to their potassium salts/complexes; in at least one case, for the double helicate $K_2(L^3)_2$, there is structural evidence that the K^+ ions are coordinated to the poly(pyrazolyl)borate ligand.[12] The photophysical properties of the complexes of $[L^5]^-$ have been reported before but are included in the discussion here for comparison purposes because they are directly relevant.[7]

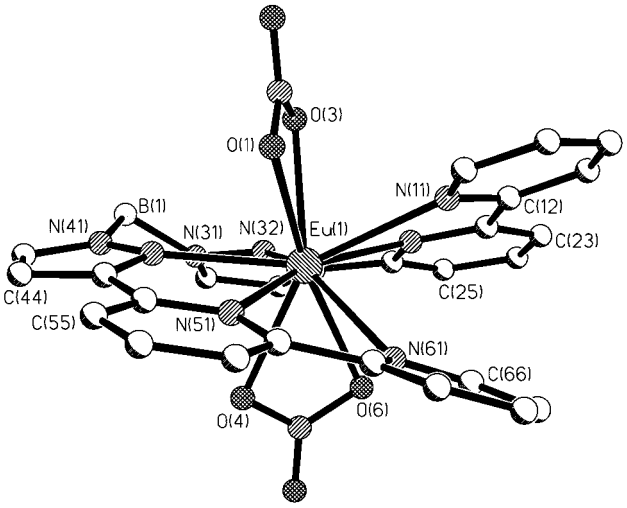

Figure 2. Crystal structure of $[Eu(L^3)(NO_3)_2]\cdot dmf\cdot 0.5Et_2O$.

All of the complexes investigated here are thermally stable in CH_2Cl_2 and MeOH; in H_2O however only the $[L^4]^{2-}$ series displays good stability. The free ligands (as their potassium salts) are relatively stable only in CH_2Cl_2. In Figure 5 the absorption spectra of all the investigated Tb^{3+} complexes are reported; Eu^{3+} and Gd^{3+} analogues exhibit almost identical spectral profiles. It is important to recall that lanthanide ions do not appreciably contribute to the spectra of their complexes since f−f transitions

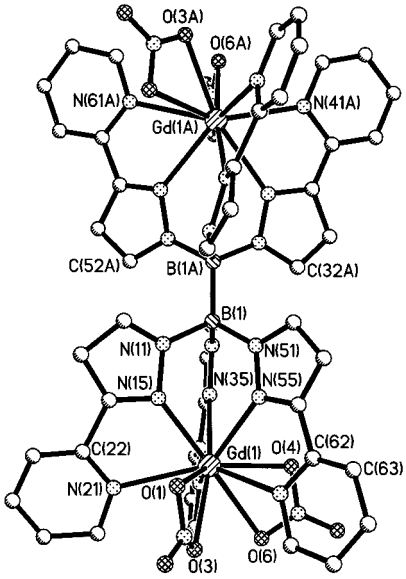

Figure 3. Crystal structure of $[\{Gd(NO_3)_2\}L^4]\cdot 2.4dmf$. Only the major component of the disorder, involving the position of one of the chelating arms and one of the nitrate ions, is shown.

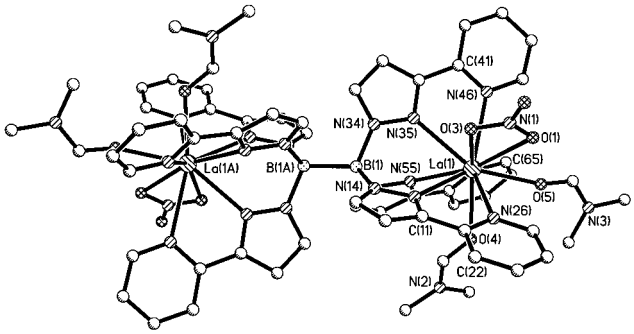

Figure 4. Crystal structure of $[\{La(NO_3)(dmf)_2\}_2(L^4)](NO_3)_2\cdot dmf$.

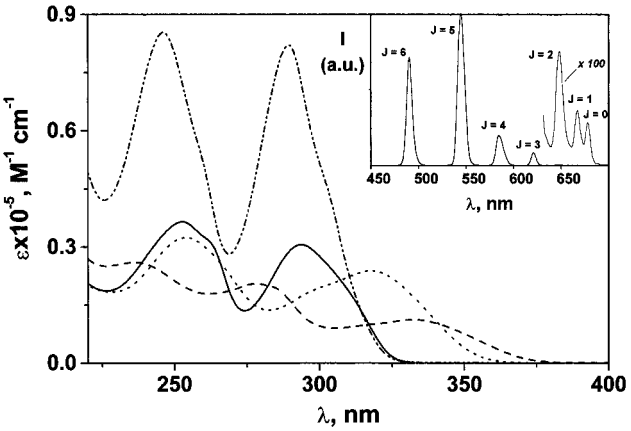

Figure 5. Absorption spectra of $Tb\cdot L^1$ (—), $Tb\cdot L^2$ (···), $Tb\cdot L^3$ (- - -), and $Tb_2\cdot L^4$ (- ·· -) in MeOH at 298 K. Inset: luminescence spectrum of $Tb\cdot L^1$ under the same conditions; the narrow bands correspond to the $^5D_4 \rightarrow {}^7F_J$ transitions ($J = 0-6$).

are Laporte-forbidden and very weak (extinction coefficients of the order of only 0.5−3.0 M^{-1} cm^{-1}); on the other hand, charge-transfer bands involving lanthanide orbitals are also typically not observed in the near-UV and visible spectral regions.[18] Hence the absorption bands of lanthanide complexes are completely attributable to ligand-centered (LC) transitions

(18) Sabbatini, N.; Guardigli, M.; Lehn, J.-M. *Coord. Chem. Rev.* **1993**, *123*, 201.

Table 4. Selected Bond Distances (Å) and Angles (deg) for $[Eu(L^3)(NO_3)_2]\cdot dmf\cdot 0.5Et_2O$

Eu(1)−O(1)	2.503(4)	Eu(1)−N(21)	2.584(5)
Eu(1)−O(3)	2.536(5)	Eu(1)−N(32)	2.507(6)
Eu(1)−O(4)	2.505(4)	Eu(1)−N(42)	2.518(6)
Eu(1)−O(6)	2.609(5)	Eu(1)−N(51)	2.602(5)
Eu(1)−N(11)	2.685(6)	Eu(1)−N(61)	2.657(6)
O(1)−Eu(1)−O(3)	50.7(2)	N(51)−Eu(1)−N(61)	61.1(2)
O(4)−Eu(1)−O(6)	49.7(2)	N(21)−Eu(1)−N(11)	61.1(2)
N(32)−Eu(1)−N(21)	63.0(2)	N(32)−Eu(1)−N(11)	119.6(2)
N(42)−Eu(1)−N(51)	64.4(2)	N(42)−Eu(1)−N(61)	123.2(2)

Table 5. Selected Bond Distances (Å) for the Structures of $[\{Gd(NO_3)_2\}_2(L^4)]\cdot 2.4dmf$ and $[\{La(NO_3)(dmf)_2\}_2(L^4)](NO_3)_2\cdot dmf$

Gd(1)−O(1)	2.52(4)[a]	La(1)−O(1)	2.716(2)
Gd(1)−O(1′)	2.57(3)[b]		
Gd(1)−O(3)	2.45(3)[a]	La(1)−O(3)	2.637(2)
Gd(1)−O(3′)	2.60(3)[b]		
Gd(1)−O(4)	2.47(2)	La(1)−O(4)	2.568(2)
Gd(1)−O(6)	2.54(2)	La(1)−O(5)	2.507(2)
Gd(1)−N(15)	2.29(5)[a]	La(1)−N(15)	2.607(3)
Gd(1)−N(15′)	2.62(4)[b]		
Gd(1)−N(21)	2.65(5)[a]	La(1)−N(26)	2.695(3)
Gd(1)−N(21′)	2.66(5)[b]		
Gd(1)−N(35)	2.51(2)	La(1)−N(35)	2.645(2)
Gd(1)−N(41)	2.64(2)	La(1)−N(46)	2.763(3)
Gd(1)−N(55)	2.50(2)	La(1)−N(55)	2.638(2)
Gd(1)−N(61)	2.65(2)	La(1)−N(66)	2.789(3)

[a] Major component of disorder. [b] Minor component of disorder.

Table 6. Luminescence Properties of the Ligands and Their Gd(III) Complexes in CH_2Cl_2 (Fluid Solution at 298 K and Frozen Matrix at 77 K)

	298 K			77 K			
	^1LC[a]			^1LC[a]		^3LC[a]	
	λ_{max}, nm	τ, ns	Φ_{em}	λ_{max}, nm	τ, ns	λ_{max}, nm	τ, ms
$[L^1]^-$	353	1.5	0.280	352	2.0	444	844
$Gd\cdot L^1$	356	<0.5	0.007	356	<0.5	448	7.7
$[L^2]^-$	390	1.2	0.029	392	2.9	478	552
$Gd\cdot L^2$	383	<0.5	0.001	386	<0.5	488	7.4
$[L^3]^-$	392	2.7	0.120	374	2.2	482	840
$Gd\cdot L^3$	356	1.2	0.018	424	<0.5	490	6.5
$[L^4]^{2-}$	332	<0.5	0.005	355	0.8	*c*	*c*
$Gd_2\cdot L^4$	352	<0.5	0.004	360	<0.5	452	2.6
$[L^5]^-$ [b]	338	0.9	0.130	353	1.8	435	1140
$Gd\cdot L^5$ [b]	351	<0.5	0.002	352	<0.5	447	5.3

[a] ^1LC and ^3LC are the lowest spin-allowed and the lowest spin-forbidden ligand-centered ($\pi \rightarrow \pi^*$) excited states, respectively. [b] Data taken from ref 7 and included for comparison purposes. [c] No long-lived phosphorescence was observed; see text.

although, with respect to the corresponding free ligands, some perturbation is observable upon complexation.[7,10] In Figure 5 we see that $Tb\cdot L^2$ and $Tb\cdot L^3$ exhibit a pronounced spectral broadening toward the low-energy end of the spectrum, with significant absorption at $\lambda > 350$ nm, indicating that the pyrazinyl groups of $[L^2]^-$ and the bipyridyl groups of $[L^3]^-$ both have relatively low-lying electronic energy levels compared to the pyridyl-substituted ligands $[L^1]^-$ and $[L^4]^{2-}$. This has important consequences for the luminescence properties, as will be shown below.

Luminescence Properties of the Complexes. Free Ligands and Gd^{3+} Complexes. The compounds KL^1, KL^2, and $K_2(L^3)_2$ exhibit intense, short-lived (10^{-9} s time scale) fluorescence in CH_2Cl_2 solution which, in a rigid matrix at 77 K, is always accompanied by a strong, long-lived (10^0-10^{-1} s time scale), structured phosphorescence band (Table 6). These emissions are due to the deactivation of the lowest electronic excited singlet

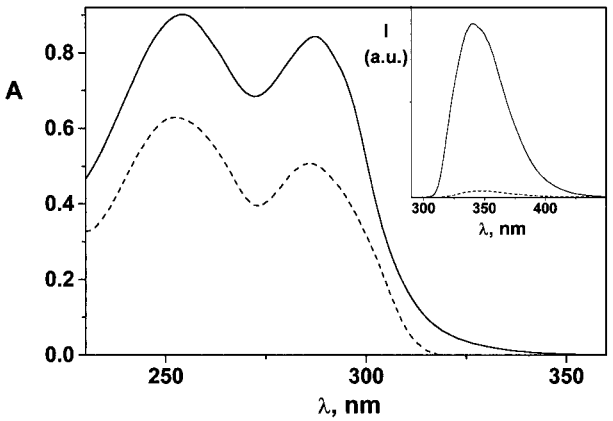

Figure 6. Absorption and (inset) fluorescence spectra of $[L^4]^{2-}$ (—) and $[L^5]^-$ (- - -) (as their K^+ salts) in CH_2Cl_2 at 298 K. Fluorescence spectra are obtained with $\lambda_{exc} = 288$ nm (same absorbance for both solutions) and clearly show the strong quenching occurring for $[L^4]^{2-}$; for more detail see the text.

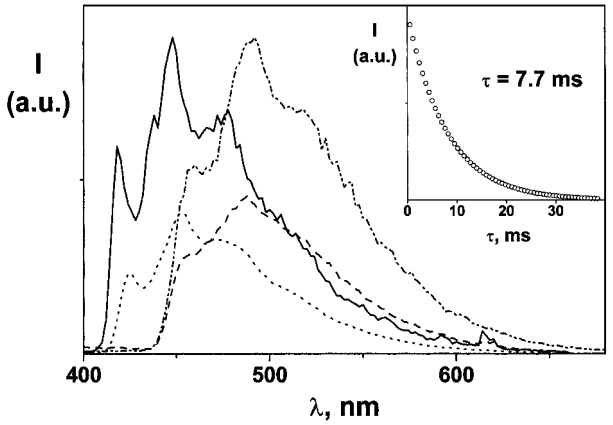

Figure 7. Phosphorescence spectra of $Gd{\cdot}L^1$ (—), $Gd{\cdot}L^2$ (···), $Gd{\cdot}L^3$ (- - -), and Gd_2L^4 (- ·· -) in CH_2Cl_2 rigid matrix at 77 K. Inset: phosphorescence decay of $Gd{\cdot}L^1$ under the same conditions; time window, 38 ms; time intervals, 1 ms; gate time, 0.8 ms.

and triplet states, respectively. K_2L^4 shows a rather peculiar behavior since the yield of fluorescence is very low, and a long-lived phosphorescence is not observed. Indeed, the absorption spectrum of K_2L^4 (Figure 6) presents a low-energy tail not observed for the similar compounds KL^1 and KL^5. This could be attributed to the presence of low-energy charge-transfer (CT) transfer states, possibly related to the dimeric nature of K_2L^4. These low-lying excited states could quench the lowest singlet and triplet states, thereby depressing or eliminating fluorescence and phosphorescence. Interestingly, the complexation of $[L^4]^{2-}$ with lanthanide ions removes this peculiarity of the ligand and, for instance, $Gd_2{\cdot}L^4$ behaves like the Gd^{3+} complexes with the other ligands.

All of the Gd^{3+} complexes show fluorescence and phosphorescence (Table 6, Figure 7), but remarkable differences can be found in the spectral position, emission quantum yields, and lifetimes with respect to the corresponding free ligands (see above for the specific case of complexes of $[L^4]^{2-}$). The decrease in the fluorescence quantum yields is due to an increase of the rate of $S_1 \rightarrow T_1$ intersystem crossing, caused by the presence of the paramagnetic Gd^{3+} ion.[19] A similar argument can explain the dramatic decrease (2 orders of magnitude) in the triplet excited-state lifetime of the Gd^{3+} complexes at 77 K, relative to the free ligands. From the highest energy vibrational feature of the phosphorescence bands (Figure 7) one can evaluate the zero−zero energy of the lowest ligand centered triplet state in the lanthanide complexes, which turns out to be 23 900, 22 100, 21 700, and 23 500 cm^{-1} for $Gd{\cdot}L^1$, $Gd{\cdot}L^2$, $Gd{\cdot}L^3$, and $Gd_2{\cdot}L^4$, respectively. These values rule out the possibility of observing metal-centered (MC) emission from the Gd^{3+} complexes since the lowest MC excited state for the Gd^{3+} ion is known to be located at much higher energy, i.e. above 31 000 cm^{-1}.[20]

Tb^{3+} and Eu^{3+} Complexes. The ligand-centered luminescence is completely suppressed in Eu^{3+} and Tb^{3+} complexes, whereas the typical narrow emission bands of the Eu^{3+} and Tb^{3+} ions can be detected upon excitation of the ligand-centered absorption bands; see for example Figure 5. The excitation spectra of all Tb^{3+} and Eu^{3+} complexes match the corresponding absorption profiles throughout the UV spectral region, showing that ligand-to-metal energy transfer takes place.[18]

Emission quantum yield and lifetime data for all the Eu^{3+} and Tb^{3+} complexes in different solvents are reported in Table 7, where the data for the previously reported complexes with $[L^5]^-$ are included for comparison.[7,10] In CH_2Cl_2 the complexes are typically stronger luminophores than in MeOH or, more markedly, in H_2O; moreover solvent deuteration usually causes a great improvement of the luminescence performances. These results are a consequence of the large nonradiative deactivation effects of the O−H oscillators of the methanol and water molecules, which interact with the first and second coordination sphere of the Ln^{3+} ion; this effect is weakened in the presence of the lower frequency O−D oscillators.[21]

At first glance, although a homogeneous family of compounds is considered, these data appear rather scattered; for instance emission quantum yield values are spread over a range of 3 orders of magnitude. A closer inspection of the luminescence data reveals several points of significance.

(i) For the complexes of $[L^1]^-$, $[L^4]^{2-}$, and $[L^5]^-$, the emission quantum yields are higher and lifetimes longer for the Tb^{3+} than for the Eu^{3+} complexes, regardless of the solvent. In contrast, this is not always the case for the $[L^2]^-$ and $[L^3]^-$ series. This behavior can be explained by taking into account that the absorption and luminescence spectra clearly show that KL^2 and $K_2(L^3)_2$ possess lower-lying electronic levels than KL^1, K_2L^4, and KL^5. Accordingly, for $Tb{\cdot}L^2$ and $Tb{\cdot}L^3$, thermally activated back-energy-transfer between the highest metal-centered $^5D_4$ level (located at 20 400 cm^{-1}) and the lowest ligand-centered triplet (^3LC), which is located just 1500 cm^{-1} above the metal-centered $^5D_4$ level (vide supra), can easily occur,[18] thus depressing the luminescence output of the metal ion. On the contrary, for $Tb{\cdot}L^1$, $Tb{\cdot}L^5$, and $Tb_2{\cdot}L^4$, the corresponding energy gap is larger than 3000 cm^{-1}, so the back-energy-transfer process to the ^3LC state is negligible and these compounds are better emitters. This thermally activated back-energy-transfer process is not so significant for the Eu^{3+} complexes, since the energy gap between the highest MC level ($^5D_1$, located at 19 000 cm^{-1} above the ground state) and the lowest ^3LC level is well above 3000 cm^{-1} in every case. Hence it is not surprising that, in CH_2Cl_2, $Eu{\cdot}L^2$ and $Eu{\cdot}L^3$ exhibit luminescence efficiency comparable to those of the other Eu^{3+} complexes homologues, unlike the Tb^{3+} complexes where the emission intensity is much more sensitive to the nature of the ligand.

(19) Bonocore, G. E.; Li, H. *Coord. Chem. Rev.* **1990**, *99*, 55.

(20) Reisfeld, R.; Jørgensen, C. K. *Lasers and Excited States of Rare Earths*; Springer: Berlin, 1977.

(21) Beeby, A.; Clarkson, I. M.; Dickins, R. S.; Faulkner, S.; Parker, D.; Royle, L.; de Sousa, A. S.; Williams, J. A. G.; Woods, M. *J. Chem Soc., Perkin Trans. 2* **1999**, *93*, 493.

Table 7. Luminescence Lifetimes and Quantum Yields of Metal-Centered Excited States in Various Solvents at 298 K

	τ, ms[a]					Φ_{em}[b]				
	CH_2Cl_2	MeOH	MeOD	H_2O	D_2O	CH_2Cl_2	MeOH	MeOD	H_2O	D_2O
Tb·L[1]	2.4	2.6	3.2	*c*	*c*	0.333	0.360	0.460	*c*	*c*
Eu·L[1]	1.7	0.8	1.9	*c*	*c*	0.003	0.002	0.021	*c*	*c*
Tb·L[2]	1.8	0.3	0.4	*d*	*d*	0.260	0.010	0.027	*d*	*d*
Eu·L[2]	1.5	0.5	1.0	*d*	*d*	0.031	0.004	0.030	*d*	*d*
Tb·L[3]	1.2	0.4	0.5	*c*	*c*	0.115	0.009	0.010	*c*	*c*
Eu·L[3]	1.9	0.9	1.5	*c*	*c*	0.046	0.018	0.085	*c*	*c*
Tb_2·L[4]	1.8	2.0	2.2	1.3	2.5	0.430	0.360	0.520	0.140	0.499
Eu_2·L[4]	1.7	0.8	1.5	0.5	2.4	0.170	0.044	0.150	0.003	0.035
Tb·L[5] [e]	2.0	1.7	2.4	0.9	2.4	0.410	0.380	0.490	0.130	0.460
Eu·L[5] [e]	1.7	0.6	1.7	0.4	2.1	0.050	0.025	0.130	0.001	0.013

[a] Measured from the most intense emission feature, i.e. $^5D_4 \rightarrow {}^7F_5$ for Tb^{3+} complexes and $^5D_0 \rightarrow {}^7F_2$ for Eu^{3+} complexes. [b] Excitation energy corresponding to lowest energy maximum of the absorption spectrum. [c] Not stable in this solvent. [d] Not well soluble in this solvent. [e] Data taken from ref 7 and included for comparison purposes.

(ii) The 10-fold difference in the luminescence quantum yields between Eu·L[1] ($\Phi = 0.003$) and Eu·L[2] ($\Phi = 0.031$) can be interpreted on the basis of the better donating properties of the pyridine nitrogen atom of $[L^1]^-$ with respect to the corresponding nitrogen of the pyrazine fragment in $[L^2]^-$, as we saw earlier from the crystallographic results. For Eu^{3+} complexes, it is well established that an important nonradiative deactivation pathway is the transfer of the ligand excitation energy to low-lying ligand-to-metal charge-transfer (LMCT) excited states; accordingly, this pathway can be favored for Eu·L[1] relative to Eu·L[2].[20] This kind of undesired radiationless deactivation is not relevant for Tb^{3+} complexes, as the reduction potential of Tb^{3+} is much higher than that of Eu^{3+}, i.e. > -3.5 and -0.35 V for the free aqua ions, respectively.[22]

(iii) The series of complexes with $[L^1]^-$, $[L^5]^-$, and $[L^4]^{2-}$ have the same type of pyrazolyl−pyridine coordinating units and display similar but not identical photophysical properties. The slightly better luminescence characteristics of Ln_2·L[4] and Ln·L[5] relative to Ln·L[1], particularly in protic solvents, suggests that the complexes Ln·L[1] are more susceptible to coordination of solvent molecules, which are known to act as effective quenchers of lanthanide luminescence via energy transfer into O−H, N−H, or C−H stretching vibrations.[21] In these 10-coordinate complexes attachment of solvent molecules must occur either by displacement of a nitrate ion,[7] as we saw above in the crystal structure of $[\{La(NO_3)(dmf)_2\}_2(L^4)](NO_3)_2$·dmf (Figure 4), by partial dissociation of the multidentate podand ligand,[8,10] or by both. The hexadentate nature of the binding sites of $[L^5]^-$ and $[L^4]^{2-}$ implies a more pronounced chelate effect than will occur for the tetradentate ligand $[L^1]^-$ and, therefore, greater resistance to partial dissociation in the presence of good donor solvents. We therefore ascribe the better luminescence properties of Ln_2·L[4] and Ln·L[5] relative to Ln·L[1] to the tripodal nature of the ligands in the former two cases, in contrast to the bipodal nature of $[L^1]^-$.[8] We note also that the Eu^{3+} complexes display a much wider variation in their emission quantum yields than do the analogous Tb^{3+} complexes. This is quite reasonable considering that Eu^{3+} is more sensitive than Tb^{3+} to nonradiative deactivation via solvent interactions, since the energy gap between the emissive and the next lower level is smaller for Eu^{3+} ($^5D_0-{}^7F_6$ gap: 12 300 cm^{-1}) than for Tb^{3+} ($^5D_4-{}^7F_0$ gap: 14 700 cm^{-1}).

(iv) The emission quantum yield of Tb·L[1] and Tb_2·L[4] in MeOD reaches the remarkable value of about 0.5. Also notable is the stability of Tb·L[5] and Tb_2·L[4] in water with luminescence quantum yields of around 0.15. These properties can be favorably compared with those of lanthanide complexes successfully employed in fluoroimmunoassay.[23]

(v) For the complexes Ln_2·L[4] one can estimate the number of water molecules coordinated to the metal center in solution n by using the equation $n = q(1/\tau_H - 1/\tau_D)$,[24] where τ_H and τ_D are the luminescence lifetimes (in milliseconds) measured in H_2O and D_2O, and the proportionality constant q is 1.05 or 4.2 ms^{-1} for Eu^{3+} or Tb^{3+}, respectively. The values obtained for Tb_2·L[4] and Eu_2·L[4] are in good agreement with one another at 1.6 in each case, with a generally accepted uncertainty of ± 0.5.[24] This is in good agreement with the crystal structure of $[\{La(NO_3)(dmf)_2\}_2L^4](NO_3)_2$ (Figure 4), which shows how loss of one nitrate ion from each metal ion can result in space for two monodentate solvent ligands.

This solvation value is smaller than we observed for the analogous mononuclear complexes Eu·L[5] and Tb·L[5] for which values of n of about 2.6 ± 0.5 were obtained,[7] although given the large error that is generally accepted for n this difference may not be very significant. However we note that in the dinuclear complexes Ln_2·L[4] replacement of one nitrate ion by two neutral solvent molecules results in a charge of +2 on the complex, whereas for the mononuclear complexes Ln·L[5] the same extent of solvation would only result in a charge of +1. There is therefore an electrostatic factor which will prevent the dinuclear complexes Ln_2·L[4] from having their nitrate ions displaced to the same extent as occurs in mononuclear complexes Ln·L,[5] in agreement with our measurements.

Conclusions

An extensive series of lanthanide(III) complexes has been prepared using multidentate podand ligands derived from poly(pyrazolyl)borates, and many of the complexes have been structurally characterized. The dinuclear complexes of $[L^4]^{2-}$, a 12-dentate ligand which binds two lanthanide ions in separate hexadentate compartments, are particularly unusual. These complexes exhibit rich and varied luminescence properties. For instance the emission quantum yield values in various solvents vary over 3 orders of magnitude, with the quantum yield values for the Tb^{3+} complexes of $[L^1]^-$, $[L^4]^{2-}$, and $[L^5]^-$ in water and methanol being among the highest reported to date.

This photophysical behavior can be rationalized on the basis of structural, electronic, and solvent-induced effects. In particular

(22) Bard, A. J. In *Standard Potentials in Aqueous Solution*; Bard, A. J., Parsons, R., Jordan, J., Eds.; Marcel Dekker: New York, 1985.
(23) Sabbatini, N.; Guardigli M.; Manet, I. In *Handbook on the Physics and Chemistry of Rare Earths*; Gschneidner, K. A., Jr., Eyring, L., Eds.; Elsevier Science: New York, 1996.
(24) Horrocks, W. DeW.; Sudnick, D. R. *Acc. Chem. Res.* **1981**, *14*, 384.

we have observed once again the role played by factors including (i) the thermally activated back-energy-transfer process between metal- and ligand-centered electronic levels for Tb^{3+} complexes, especially when low-lying electronic levels are present in the ligand, as in $Tb{\cdot}L^2$ and $Tb{\cdot}L^3$, (ii) competing energy transfer from the initially generated ^3LC excited state to an LMCT excited state in Eu^{3+} complexes, which limits the efficiency of ligand-to-metal energy transfer and thereby lowers the luminescence output of these complexes, and (iii) sensitivity of the luminescence properties to solvent-based quenching, which depends strongly on the structures of the ligands. These results, obtained for an extensive series of related compounds, clearly show a wide range of ways for tuning the absorption and luminescence properties of lanthanide complexes.

Experimental Section

Syntheses. The ligands $[L^1]^-$, $[L^2]^-$, $[L^3]^-$, and $[L^4]^{2-}$ were prepared (as their potassium salts) according to the previously published methods.[8,9,11,12] Their lanthanide complexes have the composition $[Ln(L^1)_2(NO_3)]$, $[Ln(L^2)_2(NO_3)]$, $[Ln(L^3)(NO_3)_2]$, and $[\{Ln(NO_3)_2\}_2(L^4)]$ and were all prepared simply by reaction of the ligand with 0.5 equiv (for $[L^1]^-$ and $[L^2]^-$), 1 equiv (for $[L^3]^-$), or 2 equiv (for $[L^4]^{2-}$) of the appropriate lanthanide(III) nitrate hydrate in methanol. Typically, separate solutions of the ligand and the lanthanide nitrate in the minimum amount of MeOH were prepared and then mixed together with stirring; a white precipitate formed quickly. After being stirred for 1 h, the mixture was concentrated in vacuo and cooled, and the product was filtered off, washed with a little cold MeOH, and dried to give the complexes in good yield (40−80%). Recrystallization was accomplished by slow diffusion of diethyl ether vapor into concentrated solutions of the complexes in dmf. Characterization data for the new complexes are collected in Table 1.

Crystallography. Crystals were grown by diffusion of ether vapor into concentrated solutions of the complexes in dmf; the same general procedure was used in each case. Suitable crystals were coated with hydrocarbon oil and attached to the tips of glass fibers, which were then transferred to a Siemens SMART diffractometer under a stream of cold N_2 at 173 K. A detailed description of the unit cell determination and subsequent data collection and integration using the SMART system has been published.[6] Details of the crystal parameters, data collection, and refinement for each of the structures are collected in Table 2. After collection of a full sphere of data in each case an empirical absorption correction (SADABS) was applied,[25] and the structures were then solved by conventional direct methods and refined on all F^2 data using the SHELX suite of programs on a Silicon Graphics Indy computer.[26] In all cases, non-hydrogen atoms were refined with anisotropic thermal parameters; hydrogen atoms were included in calculated positions and refined with isotropic thermal parameters which were ca. 1.2× (aromatic CH) or 1.5× (Me) the equivalent isotropic thermal parameters of their parent carbon atoms.

$[Tb(L^2)_2(NO_3)]{\cdot}$dmf and $[Gd(L^2)_2(NO_3)]{\cdot}$dmf are isostructural and isomorphous. Neither structural determination presented any problem; for $[Tb(L^2)_2(NO_3)]{\cdot}$dmf an isotropic restraint was applied to the thermal parameters of the lattice dmf molecule. The asymmetric unit of $[Eu(L^3)(NO_3)_2]{\cdot}$dmf$\cdot$0.5(Et_2O) includes a collection of closely spaced electron-density peaks close to an inversion center, which were modeled as half of a (disordered) ether molecule consisting of C(1) (100% occupancy), C(2) and C(2′) (50% occupancy each), and O (50% occupancy).

The dinuclear complex cation of $[\{La(NO_3)(dmf)_2\}_2(L^4)](NO_3)_2{\cdot}$dmf lies across an inversion center which is at the center of the B−B bond. The asymmetric unit accordingly contains half of the dinuclear complex cation, one nitrate ion, and a dmf molecule in a general position with a site occupancy of 50%; i.e., this dmf molecule is disordered equally between the two asymmetric units which make up a whole molecule.

The structural determination of $[\{Gd(NO_3)_2\}_2(L^4)]{\cdot}$2.4dmf was complicated by the small size of the crystals and the presence of extensive disorder in the structure, both of which made the data very weak; the best crystal we could find had no observable diffracted intensity above $2\theta = 40°$, and accordingly only data up to this 2θ limit were used in the refinement. The two ends of the molecule are crystallographically equivalent, with a C_2 axis through the B−B bond and perpendicular to it. In each asymmetric unit, one of the bidentate pyridyl/pyrazolyl arms, one of the nitrate ligands, and a dmf molecule are all disordered over two orientations (site occupancies 0.60/0.40). One of the dmf molecules was present in one of the disordered components (site occupancy 0.40) but absent in the other and therefore has a *total* site occupancy of 0.40. Another dmf molecule was disordered about a C_2 axis. Thus, over one-third of the atoms in the structure are disordered over two sites, and numerous restraints on the thermal parameters and geometries of the disordered components were required to keep the refinement stable. The level of refinement is accordingly modest ($R1 = 0.0107$) and the metrical parameters cannot be discussed in any detail, but the overall structure of the complex is perfectly clear.

Photophysical Studies. The solvents used for the photophysical investigations were the following: (i) spectrofluorometric grade CH_3OH and CH_2Cl_2 (Carlo Erba); (ii) triply distilled water from a Millipore Milli-RO 15 purification system; (iii) 99.5% isotopically pure CH_3OD (Aldrich) and D_2O (Carlo Erba). Absorption spectra were recorded with a Perkin-Elmer Lambda 5 spectrophotometer. Emission and excitation spectra were obtained with a Spex Fluorolog II spectrofluorimeter, equipped with a Hamamatsu R-928 photomultiplier tube. Fluorescence quantum yields were measured with the method described by Demas and Crosby,[27] using as standards $[Ru(bpy)_3]Cl_2$ ($\Phi = 0.028$ in aerated water) for the Eu^{3+} complex[28] and quinine sulfate ($\Phi = 0.546$ in 1 N H_2SO_4) for the Tb^{3+} complex.[29] The luminescence lifetimes were measured by using a Perkin-Elmer LS-50B spectrofluorometer equipped with a pulsed xenon lamp with variable repetition rate and elaborated with current software fitting procedures (Origin 5.0).

Acknowledgment. This research was supported by the European Commission COST Program D11/0004/98 "New Aspects of Supramolecular Photochemistry: from light-harvesting arrays to Molecular Machines", the Italian National Research Council (CNR), and the EPSRC (U.K.). We also thank M. Minghetti for technical assistance.

Supporting Information Available: X-ray ray data in CIF format. This material is available free of charge via the Internet at http://pubs.acs.org.

IC990708I

(25) Sheldrick, G. M. SADABS: A program for absorption correction with the Siemens SMART system, University of Göttingen, 1996.
(26) SHELXTL program system, version 5.03, Siemens Analytical X-ray Instruments, Madison, WI, 1995.
(27) Demas, J. N.; Crosby, G. A. *J. Phys. Chem.* **1971**, *93*, 2841.
(28) Nakamaru, K. *Bull. Soc. Chem. Jpn.* **1982**, *5*, 2697.
(29) Meech, S. R.; Philips, D. J. *J. Photochem.* **1983**, *23*, 193.